THE JOURNAL OF BIOLOGICAL CHEMISTRY VOL. 292, NO. 12, pp. 4913–4924, March 24, 2017
Published in the U.S.A.

Cytochrome P450 27A1 Deficiency and Regional Differences in Brain Sterol Metabolism Cause Preferential Cholestanol Accumulation in the Cerebellum*

Received for publication, December 30, 2016, and in revised form, February 10, 2017 Published, JBC Papers in Press, February 11, 2017, DOI 10.1074/jbc.M116.774760

Natalia Mast[‡], Kyle W. Anderson[§¶], Joseph B. Lin[‡], Yong Li[‡], Illarion V. Turko[§¶], Curtis Tatsuoka[‖], Ingemar Bjorkhem[**], and Irina A. Pikuleva[‡1]

*From the Departments of [‡]Ophthalmology and Visual Sciences and [‖]Neurology, Case Western Reserve University, Cleveland, Ohio 44106, the [§]Biomolecular Measurement Division, National Institute of Standards and Technology, Gaithersburg, Maryland 20899, the [¶]Institute for Bioscience and Biotechnology Research, Rockville, Maryland 20850, and the **Division of Clinical Chemistry, Department of Laboratory Medicine, Karolinska Institute, 141 86 Huddinge, Sweden*

Edited by F. Peter Guengerich

Cytochrome P450 27A1 (CYP27A1 or sterol 27-hydroxylase) is a ubiquitous, multifunctional enzyme catalyzing regio- and stereospecific hydroxylation of different sterols. In humans, complete CYP27A1 deficiency leads to cerebrotendinous xanthomatosis or nodule formation in tendons and brain (preferentially in the cerebellum) rich in cholesterol and cholestanol, the 5α-saturated analog of cholesterol. In *Cyp27a1*$^{-/-}$ mice, xanthomas are not formed, despite a significant cholestanol increase in the brain and cerebellum. The mechanism behind cholestanol production has been clarified, yet little is known about its metabolism, except that CYP27A1 might metabolize cholestanol. It also is unclear why CYP27A1 deficiency results in preferential cholestanol accumulation in the cerebellum. We hypothesized that cholestanol might be metabolized by CYP46A1, the principal cholesterol 24-hydroxylase in the brain. We quantified sterols along with CYP27A1 and CYP46A1 in mouse models (*Cyp27a1*$^{-/-}$, *Cyp46a1*$^{-/-}$, *Cyp27a1*$^{-/-}$ *Cyp46a1*$^{-/-}$, and two wild type strains) and human brain specimens. *In vitro* experiments with purified P450s were conducted as well. We demonstrate that CYP46A1 is involved in cholestanol removal from the brain and that several factors contribute to the preferential increase in cholestanol in the cerebellum arising from CYP27A1 deficiency. These factors include (i) low cerebellar abundance of CYP46A1 and high cerebellar abundance of CYP27A1, the lack of which probably selectively increases the cerebellar cholestanol production; (ii) spatial separation in the cerebellum of cholesterol/cholestanol-metabolizing P450s from a pool of metabolically available cholestanol; and (iii) weak cerebellar regulation of cholesterol biosynthesis. We identified a new physiological role of CYP46A1, an important brain enzyme and cytochrome P450 that could be activated pharmacologically.

Cholestanol (Fig. 1) is a metabolite of cholesterol, which lacks the double bond at position C5 and represents the 5α-saturated analog of cholesterol. Normally, cholestanol is present in virtually every mammalian organ at concentrations of only 1/500 to 1/800 of cholesterol (1), yet, in the disease cerebrotendinous xanthomatosis (CTX), tissue cholestanol (as well as cholesterol) is elevated, especially in the tendons and brain, where the two sterols accumulate in xanthomas, nodules rich in lipids (2, 3). In the brain, CTX xanthomas are preferentially formed in the cerebellum, in particular its white matter (4), and contain, along with the cerebellum, the highest ratios of cholestanol to cholesterol of all tissues in CTX subjects (2). Besides xanthomas, CTX is manifested by juvenile bilateral cataracts, early atherosclerosis, osteoporosis, and progressive neurological deterioration (3). CTX is an autosomal recessive disease due to deficiency in CYP27A1[2] (5, 6), a multifunctional ubiquitous cytochrome P450 enzyme involved in the production of bile acid intermediates in the liver, cholesterol elimination from extrahepatic tissues, and metabolism of vitamin D_3 in the kidney (7, 8).

The major pathway for cholestanol production in the CTX brain is established (Fig. 1) and accounts for about 70% of the synthesis of this steroid (9, 10). This pathway begins in the liver, where 7α-hydroxy-4-cholesten-3-one, an efficient precursor to cholestanol in various tissues, cannot be metabolized by CYP27A1 (11, 12) and is therefore released in the systemic circulation (13). From the circulation, 7α-hydroxy-4-cholesten-3-one is continuously fluxed across the blood-brain barrier to the brain (4, 14, 15) for the conversion to cholesta-4,6-dien-3-one, 4-cholesten-3-one, 5α-cholestan-3-one, and finally cholestanol (10, 14, 16–19). Remarkably, a flux of only 2% of 7α-hydroxy-

* This work was supported in part by National Institutes of Health Grant GM62882 (to I. A. P) and P30 Core Grant EY011373. The authors declare that they have no conflicts of interest with the contents of this article. The content is solely the responsibility of the authors and does not necessarily represent the official views of the National Institutes of Health. Certain commercial materials, instruments, and equipment are identified in this manuscript in order to specify the experimental procedure as completely as possible. In no case does such identification imply a recommendation or endorsement by the National Institute of Standards and Technology nor does it imply that the materials, instruments, or equipment identified are necessarily the best available for the purpose.

[1] To whom correspondence should be addressed: Dept. of Ophthalmology and Visual Sciences, Case Western Reserve University, 2085 Adelbert Rd., Cleveland, OH 44106. Tel.: 216-368-3823; Fax: 216-368-0763; E-mail: iap8@case.edu.

[2] The abbreviations used are: CYP, cytochrome P450; CTX, cerebrotendinous xanthomatosis; HPCD, 2-hydroxypropyl-β-cyclodextrin; MRM multiple reaction monitoring; HMGCR, 3-hydroxy-3-methylglutaryl-CoA reductase.

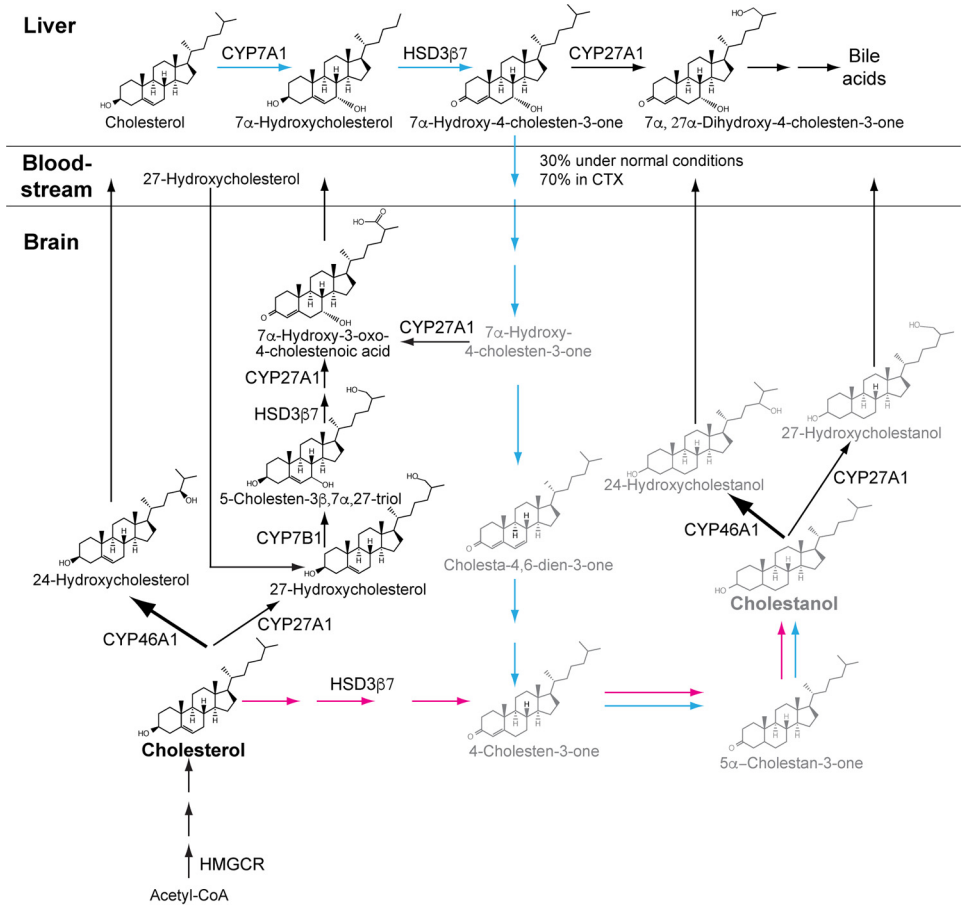

FIGURE 1. **Proposed pathways of cholestanol biosynthesis and elimination from the brain.** The 7α-hydroxy-4-cholesten-3-one-dependent pathway is initiated in the liver and is indicated with *blue arrows*; cholestanol precursors and metabolites in this pathway are shown in *gray*. The cholesterol-dependent pathway is initiated in the brain and is indicated with *magenta arrows*. In both pathways, the known enzymes are indicated; *boldface arrows* represent the major mechanism for cholesterol or cholestanol elimination from the brain.

4-cholesten-3-one and other 7α-hydroxylated sterols into the brain is sufficient to explain cerebral accumulation of cholestanol in CTX (4). However, under normal conditions, the 7α-hydroxy-4-cholesten-3-one-dependent pathway accounts for only about 30% of cholestanol biosynthesis in the brain, and cerebral cholestanol is mainly formed from cholesterol, which is synthesized locally and is oxidized to 4-cholesten-3-one (Fig. 1). The details of this oxidation have not yet been clarified but were suggested to include a microsomal 3β-hydroxy-Δ^5-dehydrogenase reaction (16). A non-enzymatic cholesterol oxidation in the brain was also reported by the amyloid-β-peptide·Cu^{2+} complex (20) and potentially could be of importance. Amyloid-β plaques are already detected in human brain at the age of 30, and their accumulation progresses with age (21).

The present work was initiated by the ophthalmic characterization of *Cyp27a1*$^{-/-}$*Cyp46a1*$^{-/-}$ mice, whose cholestanol was found to be elevated in the retina (22), a neural tissue in the back of the eye and a part of the CNS. We hypothesized that this sterol increase could be due to cholestanol metabolism by CYP46A1 and decided to investigate whether cholestanol is also increased in the brain of *Cyp27a1*$^{-/-}$*Cyp46a1*$^{-/-}$ mice. CYP46A1 is a CNS-specific enzyme, which catalyzes cholesterol 24-hydroxylation, the major mechanism for cholesterol elimination from the brain (23, 24). Unlike cholesterol, which cannot cross the blood-brain barrier, 24(*S*)-hydroxycholesterol rapidly diffuses to the systemic circulation and is delivered to the liver for further degradation to bile acids (23). CYP46A1 is more abundant in the brain than ubiquitous CYP27A1 (25). Therefore, the regional brain concentrations of 27-hydroxycholesterol, the primary CYP27A1 product, are much lower than those of 24-hydroxycholesterol. They represent only ~10–20% of the brain 24-hydroxycholesterol content (23), despite there being substantial uptake by the brain of extracerebral 27-hydroxycholesterol from the systemic circulation (26). Once in the brain, 27-hydroxycholesterol, blood-borne or synthesized locally, is further metabolized to 7α-hydroxy-3-oxo-4-cholestenoic acid (Fig. 1), which is then effluxed into the systemic circulation (27).

Similar to CTX, cholestanol is elevated in the plasma, tendons, and brain of *Cyp27a1*$^{-/-}$ mice and probably has the same mechanism of tissue accumulation (10), yet cholestanol increases are lower in *Cyp27a1*$^{-/-}$ mice as compared with CTX-affected individuals, and these animals do not develop xanthomas (13, 28, 29). Nevertheless, *Cyp27a1*$^{-/-}$ mice provide valuable mechanistic insights into the etiology of CTX (10). Accordingly, these as well as other genetically manipulated animals were used in the present work along with the brain tissues from human donors. We identified several factors that probably underlie the preferential cholestanol accumulation in CYP27A1 deficiency.

Results

Cholesterol and Cholestanol Concentrations in Mouse and Human Brain—The specimens characterized were from two background wild type strains (C57BL/6J and C57BL/6J;129S6/SvEv), three knock-out lines (*Cyp27a1*$^{-/-}$, *Cyp46a1*$^{-/-}$, and *Cyp27a1*$^{-/-}$*Cyp46a1*$^{-/-}$), and two human donors (one female and one male). In the whole mouse brain (Fig. 2*A*), the levels of cholesterol were unchanged in all genotypes. In contrast, the levels of the whole brain cholestanol varied and were increased in the knock-out strains. In *Cyp27a1*$^{-/-}$ mice, the cholestanol increases were 9.9-fold in females and 7.6-fold in males, a pattern consistent with previous work (10). In the *Cyp46a1*$^{-/-}$ genotype, cholestanol was not changed in females and was increased 4.5-fold in males with the gender difference being statistically significant. Finally, *Cyp27a1*$^{-/-}$*Cyp46a1*$^{-/-}$ mice had the highest increase in the whole brain cholestanol, 11.6-fold in females and 8.3-fold in males. Thus, in *Cyp27a1*$^{-/-}$*Cyp46a1*$^{-/-}$ mice, not only the retina but also the whole brain had an increase in cholestanol (22). Furthermore, in the wild type strains, the whole brain cholestanol represented 0.06–0.07% of cholesterol, whereas in the knock-out strains, the cholestanol to cholesterol percentages were higher: 0.51–0.68% in *Cyp27a1*$^{-/-}$ mice, 0.11–0.33% in *Cyp46a1*$^{-/-}$ mice, and 0.6–0.7% in *Cyp27a1*$^{-/-}$*Cyp46a1*$^{-/-}$ mice.

Next, we carried out the measurements in mouse and human cerebella. In the wild type strains, the basal cerebellar levels of cholesterol and cholestanol were higher than those in the whole brain: 376–544 *versus* 278–360 nmol/mg of protein for cholesterol and 983–1,581 *versus* 175–237 pmol/mg of protein for cholestanol (Fig. 2*B*). The content of cholestanol relative to cholesterol was also higher than that in the whole brain (0.25–0.31% *versus* 0.06–0.07%). Similarly, the cerebellar cholestanol to cholesterol percentages in the knock-out strains were higher than those in the whole brain: 2.1–2.3% in *Cyp27a1*$^{-/-}$ mice, 0.3–0.4% in *Cyp46a1*$^{-/-}$ mice, and 2.7–2.9% in *Cyp27a1*$^{-/-}$*Cyp46a1*$^{-/-}$ mice. These percentages were also higher relative to those in the cerebellum of the corresponding wild types.

Cerebellar specimens from only two human donors, one female and one male, were analyzed. Hence, the data obtained do not allow generalizations and are interpreted with extreme caution. Nevertheless, these data provide valuable insight into interspecies similarities and difference for cerebellar sterol and P450 content. In human cerebellum (Fig. 2*C*), cholesterol content in the gray matter seemed to be >1.6-fold lower than that in the white matter (392–400 *versus* 654–667 nmol/mg of protein) and appeared to be comparable with the cholesterol content in the cerebellum of wild type mice (376–540 nmol/mg of protein). In contrast, the cerebellar gray matter cholestanol seemed to be >1.7-fold higher than that in the white matter (900–924 and 500–542 nmol/mg of protein, respectively) but appeared to be similar to cholestanol content in the whole mouse cerebellum (980–1580 pmol/mg of protein). In our two donors, cholestanol represented 0.22–0.23% of cholesterol in the cerebellar gray matter and 0.08% of cholesterol in the cerebellar white matter, thus revealing that the sterol profile of the human cerebellar gray matter could be more similar to that of the whole mouse cerebellum than the white matter.

Cholestanol and 7α-Hydroxy-4-cholesten-3-one Concentrations in Mouse Plasma and Brain—In CYP27A1 deficiency, plasma 7α-hydroxy-4-cholesten-3-one is increased in humans and mice and underlies subsequent cholestanol accumulation in the brain (10). We investigated whether this is the case for the *Cyp46a1*$^{-/-}$ and *Cyp27a1*$^{-/-}$*Cyp46a1*$^{-/-}$ genotypes. Both cholestanol and 7α-hydroxy-4-cholesten-3-one were unchanged in the plasma of *Cyp46a1*$^{-/-}$ mice but increased in the plasma of *Cyp27a1*$^{-/-}$*Cyp46a1*$^{-/-}$ mice, by 2.2–2.8- and 45–48-fold, respectively (Fig. 3, *A* and *B*); the plasma of *Cyp27a1*$^{-/-}$*Cyp46a1*$^{-/-}$ mice had cholestanol and 7α-hydroxy-4-cholesten-3-one increases comparable with those in the plasma of *Cyp27a1*$^{-/-}$ mice (2.1–2.2- and 38–55-fold, respectively). Thus, in the brain, the mechanism of cholestanol accumulation is probably unique in *Cyp46a1*$^{-/-}$ mice and similar in *Cyp27a1*$^{-/-}$ and *Cyp27a1*$^{-/-}$*Cyp46a1*$^{-/-}$ animals. The measurements in the brain revealed that in *Cyp46a1*$^{-/-}$ mice, the 7α-hydroxy-4-cholesten-3-one levels were similar to those of the wild type mice in the whole brain but not the cerebellum (Fig. 3, *C* and *D*). In *Cyp27a1*$^{-/-}$ and *Cyp27a1*$^{-/-}$*Cyp46a1*$^{-/-}$ mice, the levels of this metabolite were decreased relative to the wild type concentrations both in the whole brain and cerebellum. This effect was higher in the whole brain than in the cerebellum, suggesting that the cerebellar metabolism of 7α-hydroxy-4-cholesten-3-one is not as efficient as that in the other brain regions. Furthermore, in the whole brain, the decreases in the levels of 7α-hydroxy-4-cholesten-3-one were higher in *Cyp27a1*$^{-/-}$ mice (7.4–9.0-fold) than in *Cyp27a1*$^{-/-}$*Cyp46a1*$^{-/-}$ mice (4.0–4.5-fold), whereas in the cerebellum, the two genotypes had comparable decreases in the levels of 7α-hydroxy-4-cholesten-3-one (1.7–2.6-fold in *Cyp27a1*$^{-/-}$ mice and 2.7–3.4-fold in *Cyp27a1*$^{-/-}$*Cyp46a1*$^{-/-}$ mice).

Cholestanol Is the Substrate for CYP46A1 in Vitro—Cholestanol, which is structurally very similar to cholesterol, was previously found to undergo 24-hydroxylation when incubated with *CYP46A1*-transfected HEK293 cells (30). However, the yield of the product was low, precluding its detailed characterization by mass spectrometry. In the present work, we used the *in vitro* reconstituted system and incubated cholestanol with purified recombinant CYP46A1. The incubation times varied and were 30 and 60 min; the product formation was assessed by gas chromatography-mass spectrometry (GC-MS). Only one peak, eluted at 29.46 min during GC, showed the expected intensity increase with the incubation time (Fig. 4*A*). This peak was not seen in the control incubations lacking NADPH and had a fragmentation pattern consistent with that of 24-hydroxycholestanol with the characteristic *m/z* values of 533 (M-15), 415 (M-90-43), and 325 (M-90-90-43) (Fig. 4*B*). Thus, cholestanol is metabolized by CYP46A1 *in vitro*. Cholestanol was next characterized in the spectral assay and compared with cholesterol for binding to CYP46A1. Both sterols had nanomolar apparent spectral K_d values (Table 1), revealing tight P450 binding. The apparent K_d of cholestanol was ~70 nM, suggesting that in our enzyme assay, 50 μM cholestanol was probably saturating for CYP46A1. Hence, we could estimate the turnover number of cholestanol in the 30-min incubation (0.04 min^{-1}) and found that it was comparable with that of cholesterol (0.11 min^{-1}) (31).

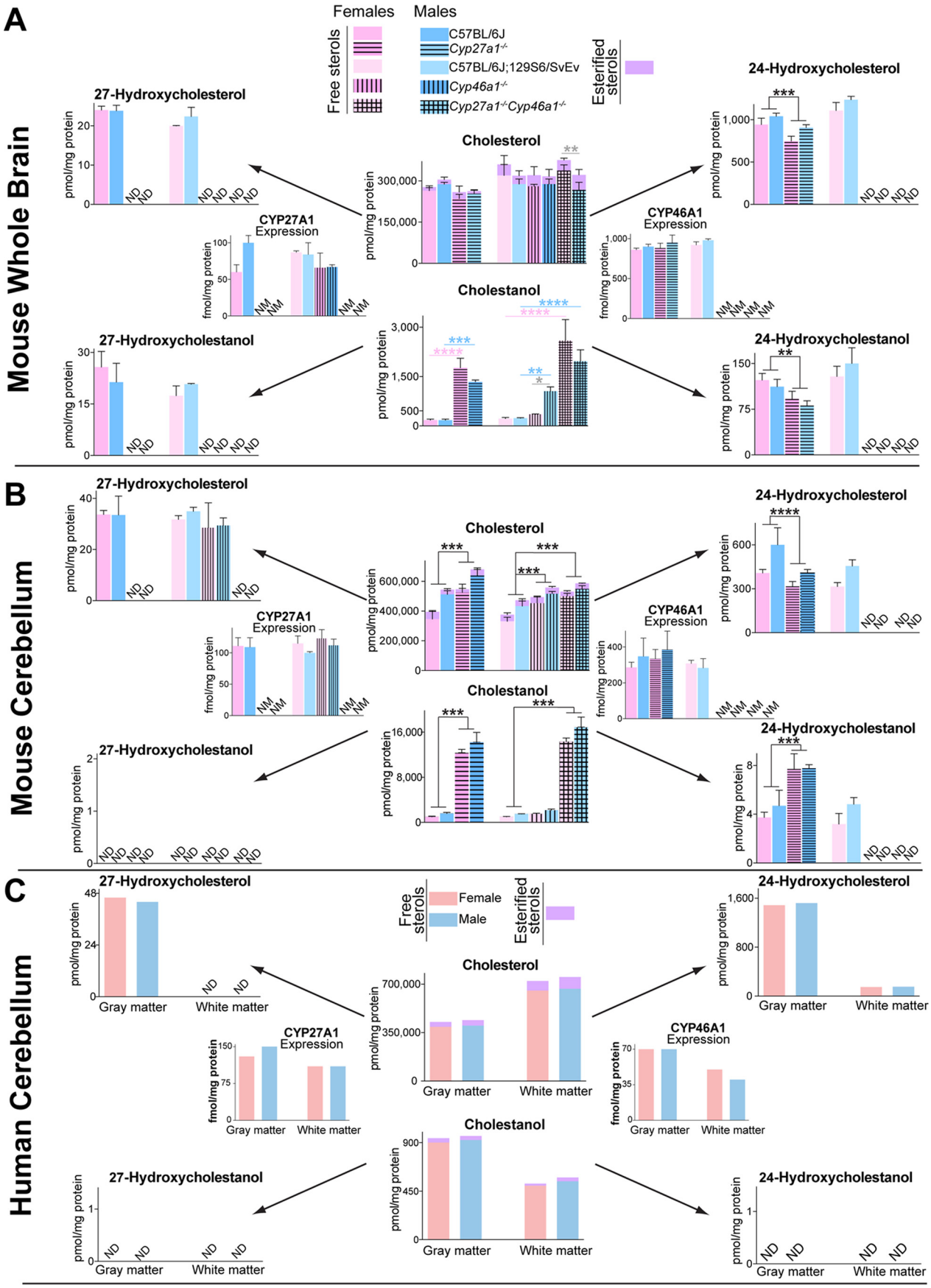
A
Mouse Whole Brain
Females
Males
Free sterols
C57BL/6J
Cyp27a1-/-
C57BL/6J;129S6/SvEv
Cyp46a1-/-
Cyp27a1-/-Cyp46a1-/-
Esterified sterols
27-Hydroxycholesterol
Cholesterol
24-Hydroxycholesterol
CYP27A1 Expression
CYP46A1 Expression
Cholestanol
27-Hydroxycholestanol
24-Hydroxycholestanol
pmol/mg protein
fmol/mg protein
ND
NM
B
Mouse Cerebellum
C
Human Cerebellum
Female
Male
Gray matter
White matter

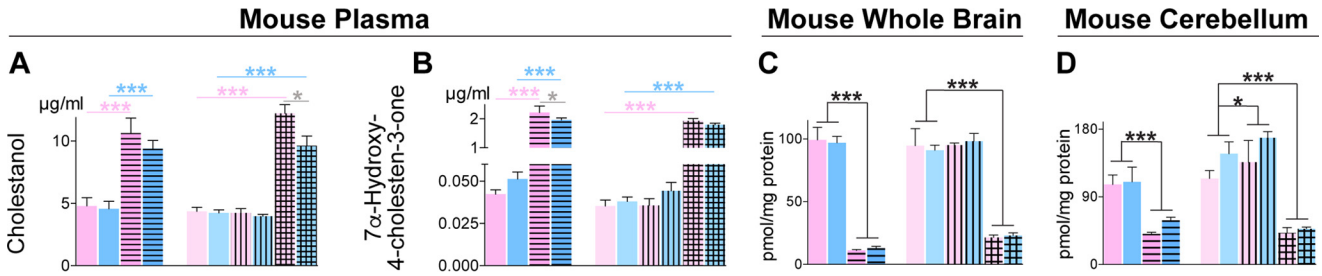

FIGURE 3. **Levels of cholestanol and 7α-hydroxy-4-cholesten-3-one in mouse plasma and brain.** The results are mean ± S.D. of the independent measurements in five mice per genotype and gender (*A–C*) or three mice per genotype and gender (*D*). The *bar fill pattern*, *color codes* for *bars*, statistical analysis, and *asterisks* as well as *p* values are the same as in Fig. 2.

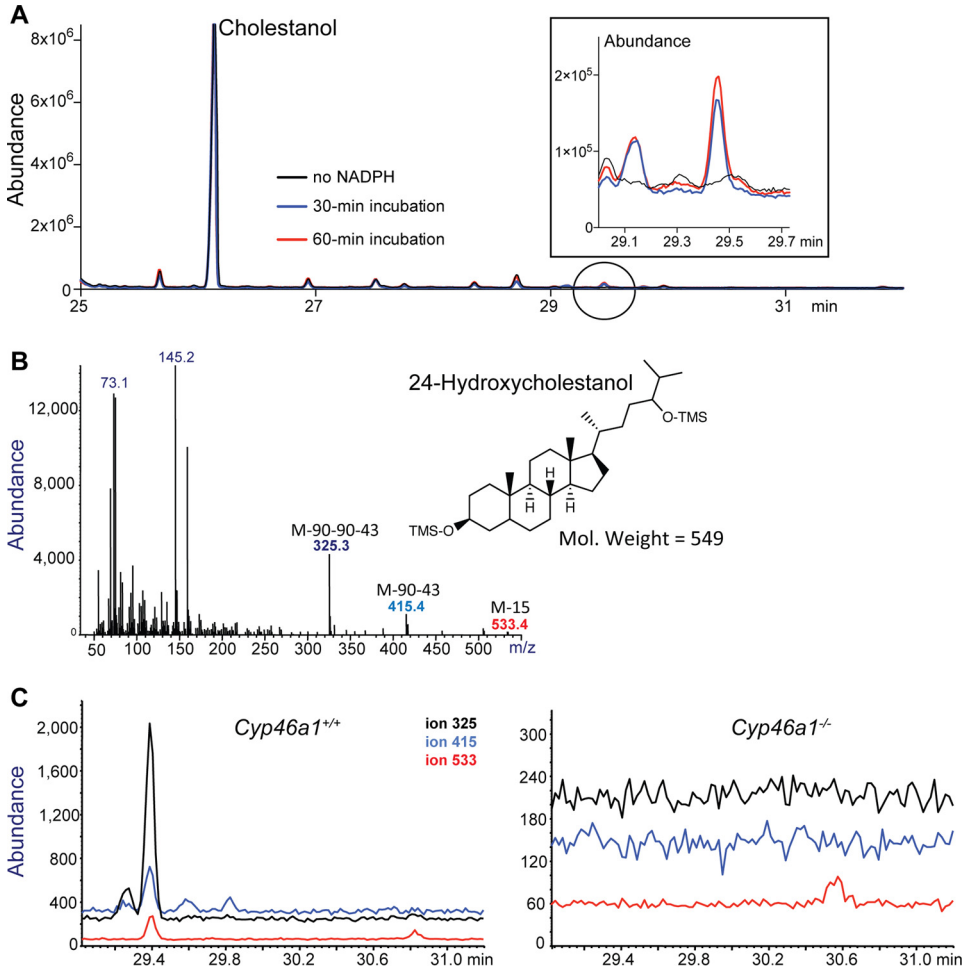

FIGURE 4. **Cholestanol is an endogenous substrate for CYP46A1 in mice.** *A*, total ion chromatogram of sterol extract (after trimethylsilylation) from the *in vitro* incubations of cholestanol with purified recombinant CYP46A1. The peak at 29.46 min corresponding to the CYP46A1 product is *circled* and shown as an *inset*. *B*, mass spectrum of the peak at 29.46 min is consistent with the fragmentation pattern of 24-hydroxycholestanol. *C*, single ion monitoring chromatogram of the oxysterol fraction isolated from the whole brain of wild type (*Cyp46a1*$^{+/+}$) and *Cyp46a1*$^{-/-}$ mice.

When a 1:1 mixture of cholesterol and cholestanol was used in the *in vitro* reconstituted system, purified recombinant CYP27A1 hydroxylated cholestanol as well (32). Herein, we used only one sterol, cholestanol, and the CYP27A1 *in vitro* enzyme assay was run for 5 and 15 min. As in incubations with CYP46A1, only one product peak, eluted at 30.96 min,

FIGURE 2. **Brain levels of CYP27A1, CYP46A1, and their substrates and metabolites.** For sterol quantifications, the results are the mean ± S.D. of the independent measurements in five mice per genotype and gender (*A*), three mice per genotype and gender (*B*), or duplicate measurements in the specimens from one female and one male donor (*C*). *ND*, not detected (the limit of detection is 1 pmol/mg of protein). MRM data from 3–4 transitions/peptide (3 peptides for CYP46A1 and 2 peptides for CYP27A1) were combined to determine the amount of each P450. Data represent mean ± S.D. (error bars) of the independent P450 measurements in three mice or one human donor. *NM*, not measured. *Pink asterisks*, significant changes between females of the knock-out strains *versus* females of the corresponding wild type strain. *Blue asterisks*, significant changes between males of the knock-out strains and males of the corresponding wild type strain. *Gray asterisks*, significant changes between female and male mice of the same strain. *Black asterisks*, significant changes between the genotypes when data were collapsed across genders. *, $p \leq 0.05$; **, $p \leq 0.01$; ***, $p \leq 0.001$; ****, $p \leq 0.0001$ by two-way analysis of variance followed by Bonferroni correction as described under "Experimental Procedures."

increased with reaction time (Fig. 5*A*), and this peak had a fragmentation pattern (Fig. 5*B*) consistent with that of 27-hydroxycholestanol reported previously (32). The turnover number for a 5-min incubation was estimated (3.5 min^{-1}) and appeared to be similar to that of cholesterol (3.0 min^{-1}) (33). The spectral parameters of cholestanol and cholesterol binding to CYP27A1 were also similar, with apparent spectral K_d values of 5.0 and 6.3 μM, respectively (Table 1). Thus, under the optimal conditions of the *in vitro* assays, cholestanol binding to CYP46A1 and CYP27A1 and subsequent metabolism by the P450s were comparable with those of cholesterol.

TABLE 1

Spectral binding of cholesterol and cholestanol to CYP27A1 and CYP46A1

Titrations were carried out as described under "Experimental Procedures."

P450	Ligand	K_d[a]	ΔA_{max}
		μM	
CYP27A1	Cholestanol	5.0 ± 0.6	0.064 ± 0.009
	Cholesterol	6.3 ± 0.7	0.034 ± 0.004
CYP46A1	Cholestanol	0.07 ± 0.03[b]	0.041 ± 0.001
	Cholesterol	0.05 ± 0.03[b]	0.047 ± 0.002

[a] All results represent mean ± S.D. of three titrations.
[b] These K_d values are much lower than the CYP46A1 concentration in the assay; hence, they represent estimates only and reflect whether the substrate has low, intermediate, or high nanomolar affinity for CYP46A1.

Cholestanol Is the Substrate for CYP46A1 in Mice—Because cholestanol was metabolized by CYP46A1 *in vitro*, mouse and human brains were analyzed for 24-hydroxycholestanol, the P450 enzymatic product. The ion peaks characteristic of 24-hydroxycholestanol were indeed detected in the whole brain of wild type mice but not in *Cyp46a1*$^{-/-}$ mice (Fig. 4*C*), providing evidence that cholestanol is the substrate for CYP46A1 *in vivo*. The ion peaks characteristic of 27-hydroxycholestanol (Fig. 5*C*) were found in the whole brain of wild type mice as well, yet they were not observed in *Cyp27a1*$^{-/-}$ mice, further support that cholestanol is metabolized by CYP27A1 *in vivo* (32). 24- and 27-hydroxycholestanols were then quantified in mouse and human brains and compared with the levels of 24- and 27-hydroxycholesterols, which were also measured. In wild type mice, the content of 24-hydroxycholestanol was much lower than that of 24-hydoxycholesterol, by ~8-fold in the whole brain and >100-fold in the cerebellum, yet the percentage ratios of 24-hydroxycholestanol to cholestanol and 24-hydroxycholesterol to cholesterol were comparable (0.1–0.4%),

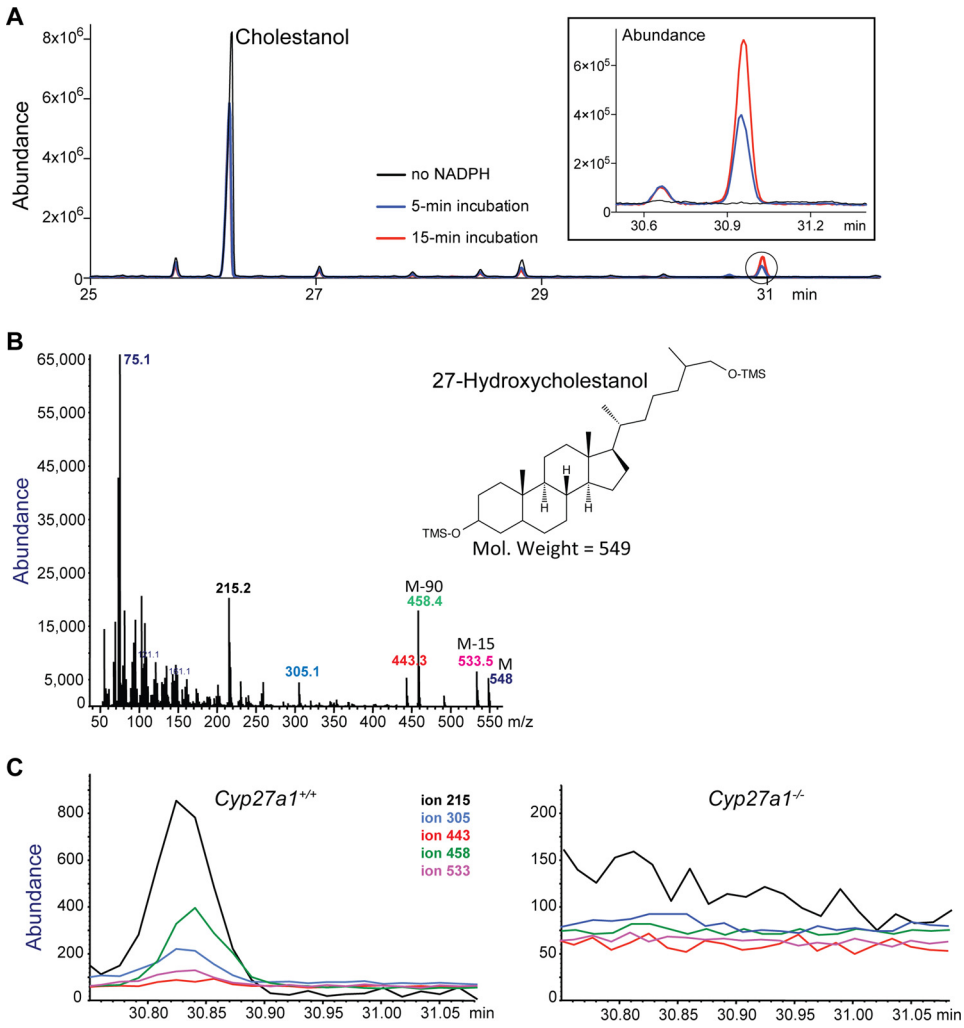

FIGURE 5. **Cholestanol is an endogenous substrate for CYP27A1 in mice.** *A*, total ion chromatogram of sterol extract (after trimethylsilylation) from the *in vitro* incubations of cholestanol with purified recombinant CYP27A1. The peak at 30.96 min corresponding to the CYP27A1 product is *circled* and shown as an *inset*. *B*, mass spectrum of the peak at 30.96 min is consistent with the fragmentation pattern of 27-hydroxycholestanol. *C*, single ion monitoring chromatogram of the oxysterol fraction isolated from the whole brain of wild type (*Cyp27a1*$^{+/+}$) and *Cyp27a1*$^{-/-}$ mice.

except 58–68% of 24-hydroxycholestanol relative to cholestanol in the whole brain. 27-Hydroxycholestanol was detected in the whole brain of wild type mice (17–26 pmol/mg of protein) but not in the cerebellum and was at levels similar to those of the whole brain 27-hydroxycholesterol (18–32 pmol/mg of protein). The content of the whole brain 27-hydroxycholestanol was 10–15% of that of cholestanol, which is much lower than the percentage content of 24-hydroxycholestanol to cholestanol (58–68%). Thus, the cerebellum does not appear to be very efficient in the metabolism of cholestanol, which is mostly hydroxylated in the other brain regions, more by CYP46A1 than by CYP27A1.

Neither 24- nor 27-hydroxycholestanol seemed to be detected in human cerebellar gray and white matter (Fig. 2*C*), yet 24- and 27-hydroxycholesterols were present, at much higher concentrations in the gray matter than in the white matter, the pattern of 27-hydroxycholesterol distribution different from that found in the previous work (26). This could be due to the post-mortem sterol washout (34) and small amounts of tissue 27-hydroxycholesterol. Remarkably, of all of the brain specimens analyzed, human or mouse, the levels of 24-hydroxycholesterol and 27-hydroxycholesterol appeared to be the highest in the human cerebellar gray matter (1487–1521 and 44–46 pmol/mg of protein, respectively). Hence, CYP46A1 and CYP27A1 expression was measured, which could contribute to tissue differences in the amounts of hydroxylated sterols.

P450 Expression in the Brain—The highest CYP46A1 expression was in the mouse whole brain (860–980 fmol/mg of protein; Fig. 2*A*); the lowest seemed to be in human cerebellum (40–70 fmol/mg of protein; Fig. 2*C*), with mouse cerebellum having intermediate P450 expression (283–383 fmol/mg of protein; Fig. 2*B*). Notably, in human cerebellum, CYP46A1, normally a neuron-specific enzyme (35), appeared to be detected in both gray and white matter. This could be a reflection of either white matter contamination with gray matter or CYP46A1 expression in the axons of Purkinje cells and Golgi I neurons that extend deep into the cerebellum. However, the latter interpretation is not supported by the previous work on CYP46A1 immunolocalization showing no CYP46A1 expression in the axons of Purkinje cells and Golgi I neurons (35).

Unlike CYP46A1 expression, the expression of CYP27A1 seemed to be in the same range in all brain specimens except in those with enzyme deficiency (Fig. 2). In the whole mouse brain, CYP27A1 was at ~50-fold lower levels than CYP46A1, in agreement with CYP46A1 being the major cerebral cholesterol hydroxylase (23, 24). Similarly, CYP27A1 was at lower levels than CYP46A1 in mouse cerebellum. Only in human cerebellum, CYP27A1 expression appeared to be higher than that of CYP46A1 both in gray matter and white matter.

Lathosterol and Desmosterol Concentrations in Mouse Whole Brain and Cerebellum—Lathosterol and desmosterol are cholesterol precursors in the pathways of cholesterol biosynthesis and reflect the rate of cholesterol biosynthetic process in neurons (lathosterol) and astrocytes (desmosterol) (36). The rate of cholesterol biosynthesis is known to be increased in the cerebrum of *Cyp27a1*$^{-/-}$ mice, as indicated by increased lathosterol levels (10), and decreased in the whole brain of *Cyp46a1*$^{-/-}$ mice, as indicated by the balance studies (37). We

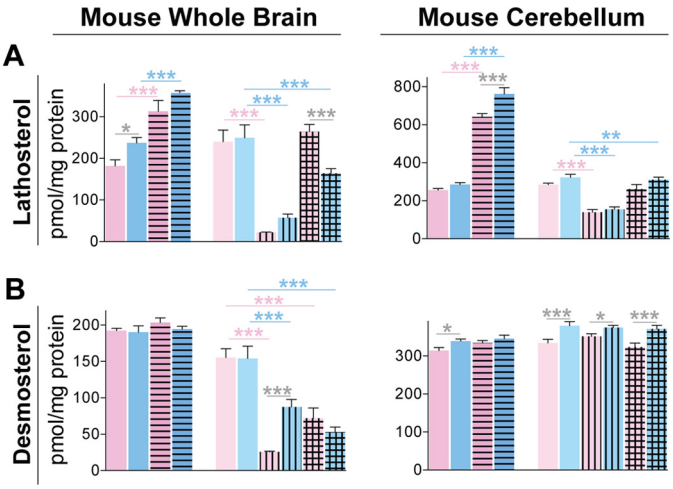

FIGURE 6. **Levels of lathosterol (*A*) and desmosterol (*B*) in mouse whole brain and cerebellum.** The results are mean ± S.D. (*error bars*) of the independent measurements in three mice per genotype and gender. The *bar fill pattern*, *color codes* for *bars*, statistical analysis, and *asterisks* as well as *p* values are the same as in Fig. 2.

investigated whether the levels of lathosterol and desmosterol were altered in the cerebellum of *Cyp27a1*$^{-/-}$, *Cyp46a1*$^{-/-}$, and *Cyp27a1*$^{-/-}$*Cyp46a1*$^{-/-}$ mice, and if so, how these changes were comparable with those in mouse whole brain. In *Cyp27a1*$^{-/-}$ mice, lathosterol was increased in both cerebellum and whole brain as compared with the corresponding wild type strain (Fig. 6*A*), and these increases were higher in the cerebellum than in the whole brain (2.5–2.7-fold *versus* 1.5–1.7-fold). In contrast, *Cyp46a1*$^{-/-}$ mice had a decrease in lathosterol levels in both cerebellum and whole brain, and these decreases were lower in the cerebellum than in the whole brain (2.1-fold *versus* 4.4–11-fold). In *Cyp27a1*$^{-/-}$*Cyp46a1*$^{-/-}$ mice, lathosterol levels were decreased in both cerebellum and whole brain, and these decreases were because of the changes in males. Desmosterol was unchanged in the cerebellum of the knock-out strains and decreased in the whole brain in *Cyp46a1*$^{-/-}$ and *Cyp27a1*$^{-/-}$*Cyp46a1*$^{-/-}$ mice (Fig. 6*B*). Thus, genetic deficiencies in CYP27A1 and CYP46A1 mainly affect cholesterol biosynthesis in brain neurons, with changes in astrocytes being pronounced only in CYP46A1-deficient strains in the whole brain. Astrocytes are believed to produce the majority of brain cholesterol (38) and, along with brain neurons, apparently have a compensatory down-regulation of cholesterol biosynthesis in the whole brain in response to a lack of cholesterol 24-hydroxylation, the major pathway of cholesterol elimination in the brain.

Discussion

The present work led to two major findings that, along with general biochemical knowledge, helped us to interpret the measurements of the sterol content and P450 expression in different brain specimens (Fig. 2). Our first finding was that not only cholesterol but also cholestanol is an endogenous substrate for CYP46A1 in the brain (Table 1 and Fig. 4). The second finding was that in mouse cerebellum, the metabolism of cholestanol is low and mainly occurs via 24-hydroxylation, whereas in the other brain regions in mice, the metabolism of cholestanol is

high and occurs via both 27- and 24-hydroxylations. In human cerebellum, cholestanol metabolism seems to be non-existent based on studies in two donors (Fig. 2*C*). It must be kept in mind that our measurements in two human samples, one from a male and one from a female, are at the moment relevant only for these two samples. While analyzing the data, we also kept in mind that enzyme and substrate concentrations as well as substrate availability and the ratio of the substrates that compete for the enzyme active site are all important biochemical factors determining the amount of the enzymatic product formed.

We established that under normal conditions (*i.e.* in wild type mice) and as compared with the whole brain and human specimens, mouse cerebellum had the highest cholestanol content (928–1582 pmol/mg of protein), the highest percentage of cholestanol relative to cholesterol (0.25–0.31%), the highest CYP27A1 expression (111–115 fmol/mg of protein), and CYP46A1 expression (286–383 fmol/mg of protein) only ~3-fold lower than that in the whole brain. Nevertheless, the wild type mouse cerebellum had the lowest 24-hydroxycholestanol concentrations (only 3–5 pmol/mg of protein) and the lowest percentage ratio of 24-hydroxycholestanol to cholestanol (0.3–0.5% for wild type mice). Conversely, the whole brain of wild type mice had the lowest cholestanol content (179–237 pmol/mg of protein) and the lowest percentage of cholestanol relative to cholesterol (0.06%-0.07%). Nevertheless, its 24-hydroxycholesterol and 24-hydroxycholestanol concentrations were the highest (112–150 and 17–26 pmol/mg of protein, respectively) as were the percentage of 24-hydroxycholestanol and 27-hydroxycholestanol to cholestanol (58–68 and 10–15%, respectively). The relatively high ratio of 24-hydroxycholestanol to cholestanol could be due to a lower rate of diffusion of 24-hydroxycholestanol from the brain into the circulation. The sterol profile of the human cerebellar gray matter appeared to be similar to that of the mouse cerebellum, except that CYP46A1 expression seemed to be much lower (only 70 fmol/mg of protein) and hydroxycholestanols were not detected, either because they were not formed or they had been washed out post-mortem. Thus, our measurements are consistent with the possibility that it is not the CYP46A1 and CYP27A1 abundance, local amounts, and ratios of cholestanol to cholesterol but rather cholestanol availability for hydroxylation that is most important for cholestanol metabolism in the brain. In addition, human CYP46A1 may have a higher catalytic efficiency of cholesterol 24-hydroxylation than the mouse ortholog. Human and mouse CYP46A1 share 95% amino acid sequence identity (24), yet many of their primary sequence differences are at the entrance or inside the CYP46A1 active site (31), the functionally important regions that could affect enzyme activity and efficiency of catalysis.

Why is cholestanol availability for CYP46A1/CYP27A1 limited (or nonexistent) in the cerebellum? There is only one cell type highly expressing CYP46A1 in the cerebellum: the somas and dendritic trees of Purkinje cells (24, 35). These cells form a single layer in the cerebellar gray matter and account for ~0.5 and 0.25% of the total neuronal content in mouse cerebellum and whole brain, respectively (39). Purkinje cells are one of the largest neurons in the brain, and CYP46A1 expression in these neurons is probably very high, as suggested by the measurable cerebellar CYP46A1 content (Fig. 2, *B* and *C*) but very low Purkinje cell content. Probably, cholestanol is either not formed/delivered to the Purkinje cells or is spatially separated in these large cells from CYP46A1, which resides in the endoplasmic reticulum. Cholestanol may also be separated from CYP27A1, a mitochondrial enzyme expressed in many cell types (40) and abundant in the cerebellum (111–115 fmol/mg of protein; Fig. 2*B*). Apparently, in the cerebellum, neither endoplasmic reticulum and mitochondria of Purkinje cells nor mitochondria of other cell types have a pool of metabolically available cholestanol. This is in contrast to cholesterol, which is available and is hydroxylated by CYP46A1 and CYP27A1 (Fig. 2, *B* and *C*). In mice, a minor cerebellar metabolism of cholestanol (24-hydroxylation) possibly takes place in Golgi cells, the granule cell layer interneurons, some of which express CYP46A1 (35). Similarly, cholestanol is probably available for CYP46A1 and CYP27A1 in the P450-containing cells of the other brain regions: in cortical and hippocampal pyramidal neurons along with hippocampal interneurons that express CYP46A1 (35) and in pyramidal neurons of the cortex as well as some cortical oligodendrocytes that express CYP27A1 (40). We suggest that there is a spatial separation of cholestanol from CYP46A1 and CYP27A1 that determines, at least in part, cholestanol accumulation in the cerebellum under the conditions of increased cholestanol load.

Other factors probably contribute to the cerebellar cholestanol accumulation in CYP27A1 deficiency. One of them could be CYP27A1 abundance, comparable with that of CYP46A1 only in the cerebellum, apparently the major site of the brain CYP27A1 expression, at least in mice (Fig. 2). Accordingly, CYP27A1 deficiency is probably affecting the cerebellum more than the other brain regions, where CYP27A1 is much less abundant because it increases the cerebellar cholestanol production. Indeed, the cerebellar 7α-hydroxy-4-cholesten-3-one, the cholestanol precursor (11, 12), cannot be metabolized in this condition by CYP27A1 and is used instead for cholestanol biosynthesis (Fig. 1).

The regulation of cholesterol biosynthesis and overproduction of cholesterol, a substrate for cholestanol biosynthesis, could be another factor that underlies cerebellar cholestanol accumulation in CYP27A1 deficiency. The possibility has been discussed that the accumulation of cholesterol in cholestanol-containing xanthomas is due to increased synthesis of cholesterol as a consequence of a lower capacity of cholestanol (as compared with cholesterol) to suppress 3-hydroxy-3-methylglutaryl-CoA reductase (HMGCR), the rate-limiting enzyme in the pathway of cholesterol biosynthesis (14). This may be part of the explanation for the increased levels of cholesterol in the cerebellum of the *Cyp27a1*$^{-/-}$ mice and *Cyp27a1*$^{-/-}$ *Cyp46a1*$^{-/-}$ mice (Fig. 2*B*). In addition, a lack of 27-hydoxycholesterol could contribute as well. Previously, we found a 12-fold increase in protein, but not mRNA, levels of HMGCR in the *Cyp27a1*$^{-/-}$ retina as compared with the wild type retina and provided an explanation (41). This increase could be a result of the 27-hydoxycholesterol-dependent HMGCR degradation because 27-hydoxycholesterol was shown to bind to the protein called INSIG (insulin-induced gene, which plays an important role in the regulation of cholesterol biosynthesis (42)) and to accelerate through this binding the degradation of

HMGCR (43). It is possible that a similar mechanism of post-translational HMGCR regulation exists in the *Cyp27a1*$^{-/-}$ brain and is stronger in the cerebellum than in the whole brain because of higher CYP27A1 abundance and levels of 27-hydoxycholesterol.

Cyp46a1$^{-/-}$ mice have unchanged levels of the whole brain cholesterol (Fig. 2*A*) because of a compensatory down-regulation of the whole brain cholesterol biosynthesis (37). Consistent with this down-regulation, lathosterol and desmosterol were significantly decreased in the whole brain of *Cyp46a1*$^{-/-}$ mice (Fig. 6). Lathosterol but not desmosterol was also decreased in the *Cyp46a1*$^{-/-}$ cerebellum but to a lower extent than in the whole brain (2.1-fold *versus* 4.4–11-fold; Fig. 6*A*). Perhaps this lower decrease was not sufficient to compensate for a lack of 24-hydroxylation; hence, the levels of cholesterol were significantly increased in the cerebellum in *Cyp46a1*$^{-/-}$ mice (Fig. 2*B*). We suggest that there may be insufficient coupling between cholesterol biosynthesis and cholesterol 24-hydroxylation in the *Cyp46a1*$^{-/-}$ cerebellum. Of interest is that in *Cyp46a1*$^{-/-}$ mice, the cerebellar cholestanol levels (1502–2146 pmol/mg of protein) were approximately equal to the sum of the wild type cerebellar cholestanol (982–1483 pmol/mg of protein) and wild type cerebellar 24-hydroxycholesterol (315–455 pmol/mg of protein). This suggests that in *Cyp46a1*$^{-/-}$ mice, a part of the cerebellar cholesterol excess formed as a result of cholesterol biosynthesis-cholesterol metabolism uncoupling was converted to cholestanol.

There seems to be at least one factor regulating cholestanol homeostasis in mouse brain, as indicated by the decreased levels of 7α-hydroxy-4-cholesten-3-one in *Cyp27a1*$^{-/-}$ and *Cyp27a1*$^{-/-}$*Cyp46a1*$^{-/-}$ mice (Fig. 3, *C* and *D*). These decreases may be considered as a compensatory up-regulation of 7α-hydroxy-4-cholesten-3-one metabolism in response to the markedly increased sterol flux from the systemic circulation in the brain. It is possible that this increased metabolism reflects an induction of the dehydratase catalyzing the first and rate-limiting step in the conversion of 7α-hydroxy-4-cholesten-3-one into cholestanol. Another possibility is that there is an induction of a hitherto unknown hydroxylase active toward 7α-hydroxy-4-cholesten-3-one. It should be emphasized that high levels of 7α-hydroxy-4-cholesten-3-one are cytotoxic (14). Hence, metabolism of 7α-hydroxy-4-cholesten-3-one, including its conversion into cholestanol, can be regarded as a detoxification.

The standard treatment for CTX is replacement therapy with chenodeoxycholic acid either alone or in combination with one of the statins, drugs that inhibit cholesterol biosynthesis (44). These pharmacologic interventions usually improve clinical symptoms and lead to stabilization of CTX, which is a slowly progressive disease. However, not all of the patients are responsive to the chenodeoxycholic acid with/without statin treatment, and some of them have progressive neurological deterioration (44). Previously, we established that CYP46A1 can be activated allosterically both *in vitro* and in mice by a very small dose of the anti-HIV drug efavirenz (45, 46). The clinical trial now is in preparation to investigate whether efavirenz activates CYP46A1 in the human brain and affects people with normal cognition and mild cognitive impairment. If successful, this trial will identify CYP46A1 as a new drug target and will suggest, along with the data of the current investigation, that pharmacologic activation of CYP46A1 should be considered not only for the treatment of people with mild cognitive impairment but also for the treatment of patients with CTX who do not respond to the treatment with chenodeoxycholic acid.

In summary, we conducted a comprehensive quantitative characterization of mouse and human brain specimens for sterol and P450 levels and revealed several factors that probably underlie the preferential cerebellar cholestanol accumulation in CYP27A1 deficiency. These factors include the ability of CYP46A1 to metabolize cholestanol, low cerebellar abundance of CYP46A1 and high cerebellar abundance of CYP27A1, spatial separation in the cerebellum of cholesterol/cholestanol-metabolizing P450s from a pool of metabolically available cholestanol, and weak cerebellar regulation of cholesterol biosynthesis. A new physiological role of CYP46A1, an important brain enzyme, was established and suggests that CYP46A1 could be not only a potential anti-Alzheimer's disease target but also a target for the treatment of CTX.

Experimental Procedures

Animals—*Cyp27a1*$^{-/-}$ mice and *Cyp27a1*$^{+/+}$ littermates were generated by crossing *Cyp27a1*$^{-/-}$ males and *Cyp27a1*$^{+/-}$ females, which in turn were obtained from the *Cyp27a1*$^{+/-}$ line provided by Dr. Sandra Erickson (University of California, San Francisco, CA). The *Cyp27a1*$^{+/-}$ line was on the C57BL/6J background (47). *Cyp46a1*$^{-/-}$ mice and *Cyp46a1*$^{+/+}$ controls were generated from *Cyp46a1*$^{+/-}$ males and females provided by Dr. David Russell (University of Texas Southwestern, Dallas, TX). This line was on the mixed C57BL/6J;129S6/SvEv background (37). Crossing *Cyp46a1*$^{+/-}$ males and females produced homozygous animals that allowed us to obtain the *Cyp46a1*$^{-/-}$ or *Cyp46a1*$^{+/+}$ breeding pairs, which established our *Cyp46a1*$^{-/-}$ and *Cyp46a1*$^{+/+}$ colonies. The *Cyp27a1*$^{-/-}$*Cyp46a1*$^{-/-}$ line and *Cyp27a*$^{+/+}$*Cyp46a1*$^{+/+}$ controls were generated by crossing *Cyp27a1*$^{-/-}$ and *Cyp46a1*$^{-/-}$ mice (22). The heterozygous animals that were produced were crossed to obtain the breeding pairs homozygous for *Cyp27a1*$^{-/-}$*Cyp46a1*$^{-/-}$ and *Cyp27a*$^{+/+}$*Cyp46a1*$^{+/+}$. These breeding pairs established our *Cyp27a1*$^{-/-}$*Cyp46a1*$^{-/-}$ and *Cyp27a*$^{+/+}$*Cyp46a1*$^{+/+}$ colonies. Animal genotyping was conducted by PCR using the genotype-specific pair of primers: 5′-CATGCGCATAGGAATGGAAAG-3′ and 5′-CATCAGTTGCATCTCCAGTTC-3′ for *Cyp27a1*$^{+/+}$; 5′-TGGTTCCCACAAACTCCCGGATCAT-3′ and 5′-ATCGCATCGAGCGAGCACGTACT-3′ for *Cyp27a1*$^{-/-}$; 5′-GGGGGCCTGGCTGGGGCTCTCGAT-3′ and 5′-CTGCCGACACATTTGTGCGGCCCAGCCAA-3′ for *Cyp46a1*$^{+/+}$; and 5′-CCTTCCTTTCCCGCCCTCCCTTGCGCTA-3′ and 5′-CTGCCGACACATTTGTGCGGCCCAGCCAA-3 for *Cyp46a1*$^{-/-}$. Animals were 4–6 months old and maintained on a standard 12-h light (~10 lux)/dark cycle. Standard rodent chow and water were provided *ad libitum*. All animals were sacrificed in the same time period, namely between 12 p.m. and 3 p.m. All animal procedures were approved by the Case Western Reserve University institutional animal care and use committee and conformed to recommen-

dations of the American Veterinary Association Panel on Euthanasia.

Human Tissues—Brain specimens were obtained during autopsy 9–11 h after death from de-identified donors following informed consent of the respective families. The brain tissue was rinsed in cold 0.9% NaCl (w/v), blotted, and immediately flash-frozen in liquid nitrogen. Samples were stored at −80 °C until further analysis. Demographic information and available medical history on donors 3 (male) and 4 (female), whose specimens were used in the present work, are described elsewhere (34). Human tissue use conformed to the Declaration of Helsinki and was qualified as "not human subjects" research by the institutional review board at the University of Texas Medical Branch.

Sterol Quantifications—Sterol quantifications were carried out as described (34, 48) by isotope dilution GC-MS using deuterated sterol analogs as internal standards. [25,26,26,26,27,27,27-$^2H_7$]24(*RS*)-Hydroxycholesterol and [25,26,26,26,27-$^2H_5$]27-hydroxycholesterol served as internal standards for 24-hydroxycholestanol and 27-hydroxycholestanol, respectively. Cholesterol and cholestanol were measured as both free and esterified forms, whereas other sterols were quantified as free forms only.

CYP27A1 and CYP46A1 Quantifications—Half of mouse brain, whole mouse cerebellum, or a portion of human cerebellum was used for sample preparation. In each case, the tissue was added to 1 ml of 25 mM ammonium bicarbonate supplemented with 1:200 (v/v) protease inhibitor mixture (Sigma-Aldrich) and sonicated twice at 10% intensity for 10 s (Sonicator 3000, Misonix Inc.). Total protein was measured using a Pierce BCA protein assay kit (Thermo Fisher Scientific), and 8 mg of each homogenate was sampled for analysis. Samples were centrifuged at 106,000 × *g* for 1 h at 4 °C. The resulting pellet was reconstituted with 25 mM ammonium bicarbonate, 2% SDS (w/v), 20 mM DTT, 7 pmol of human ^{15}N-labeled CYP46A1, 3 pmol of human ^{15}N-labeled CYP27A1. After incubation for 1 h at room temperature for reduction of cysteine residues, samples were alkylated by treatment with 55 mM iodoacetamide for 1 h. Sequential protein precipitation with a chloroform/methanol/water mixture (1:4:3, v/v/v) and then with 4 volumes of methanol was performed (49) to separate proteins from salts, lipids, and processing reagents. Precipitated protein samples were reconstituted in 25 mM ammonium bicarbonate, 0.2% sodium cholate (w/v) and digested with a 1:8 trypsin/protein ratio (w/w) overnight at 37 °C. Digested sample was quenched with 0.5% trifluoroacetic acid (v/v) and centrifuged at 106,000 × *g* for 20 min at 4 °C. Supernatant was dried using Eppendorf AG Vacufuge, and peptides were stored at −20 °C. For analysis by LC-MS, dried peptides were reconstituted in 3% acetonitrile, 97% water, and 0.1% formic acid (v/v/v). Separation was performed on an Agilent Zorbax Eclipse Plus C18 RRHD column (2.1 × 50 mm, 1.8-μm particle) coupled to an Agilent 6490 triple quadrupole mass spectrometer with iFunnel technology for multiple reaction monitoring (MRM) analysis. Peptides were eluted at a flow rate of 200 μl/min using the following gradient of solvent B in solvent A: 3% B (v/v) for 3 min, 3–30% B (v/v) in 32 min, 30–50% B (v/v) in 5 min, and 50 to 3% B (v/v) in 3 min. Solvent A was water containing 0.1% formic acid (v/v), and solvent B was acetonitrile containing 0.1% formic acid (v/v). The acquisition method had the following parameters in positive mode: fragmentor, 380 V; cell accelerator, 4 V; collision energy, 25 V; dwell, 100 ms; electron multiplier, 500 V; and capillary voltage, 3500 V. MRM transitions were predicted using Pinpoint software (Thermo Fisher Scientific) for both unlabeled and ^{15}N-labeled peptides. Precursors with +2 charge were selected for analysis. Transitions were screened in a digest of ^{15}N-labeled standard to obtain the three or four most intense transitions, which were further used for quantification (Table 2). Relative signal ratios of transitions for quantification were similar in both the ^{15}N-labeled standard digest and when standards were added into tissue homogenates, indicating no obvious interference from biological matrices on the quantification using selected transitions. Quantification was performed by calculating the ratio of peak areas for unlabeled biological peptides to labeled standard peptides using MassHunter software (Agilent) multiplying by the ratio of known fmol of standard to mg of total protein. MRM data from 3–4 transitions per peptide (3 peptides for CYP46A1 and 2 peptides for CYP27A1) were combined to determine the amount of each P450. Data represent mean ± S.D. of the independent P450 measurements in three mice or one human donor. Statistical significance of mean differences was calculated using Student's two-tailed *t* test and was considered significant if p was ≤0.05.

TABLE 2

Peptides and transitions for quantification of CYP46A1 and CYP27A1

Peptide quantifications were carried out as described under "Experimental Procedures". Transitions are listed for both unlabeled, light (L) and fully ^{15}N-labeled, heavy (H) peptides. All precursor ions were +2 charge, and product ions were +1 charge with y-ion included for reference.

P450	Peptide		Precursor (m/z)	Product ions (m/z)			
CYP46A1	LLEEETLIDGVR[h,m]	L	693.9	773.4 (y_7)	1031.5 (y_9)	1160.6 (y_{10})	
		H	701.4	783.4 (y_7)	1043.5 (y_9)	1173.5 (y_{10})	
	VLQDVFLDWAK[h,m]	L	667.4	779.4 (y_6)	993.5 (y_8)	1121.6 (y_9)	
		H	674.3	787.4 (y_6)	1003.5 (y_8)	1133.5 (y_9)	
	AEQLVEILEAK[h,m]	L	621.9	702.4 (y_6)	801.5 (y_7)	914.6 (y_8)	1042.6 (y_9)
		H	628.3	709.4 (y_6)	809.5 (y_7)	923.5 (y_8)	1053.6 (y_9)
CYP27A1	LYPVVPTNSR[h,m]	L	573.3	574.3 (y_5)	673.4 (y_6)	869.5 (y_8)	
		H	580.3	583.3 (y_5)	683.3 (y_6)	881.5 (y_8)	
	AQLQETGPDGVR[m]	L	635.8	701.4 (y_7)	830.4 (y_8)	958.5 (y_9)	1071.5 (y_{10})
		H	644.3	711.3 (y_7)	841.4 (y_8)	971.4 (y_9)	1085.5 (y_{10})
	IQHPFGSVPFGYGVR[h]	L	554.3	551.3 (y_5)	698.4 (y_6)	795.4 (y_7)	
		H	561.3	559.3 (y_5)	707.3 (y_6)	805.4 (y_7)	

[h] These peptides were used for quantifications in humans.
[m] These peptides were used for quantifications in mice.

Enzyme Assays—Recombinant human CYP27A1, human CYP46A1, bovine adrenodoxin, bovine adrenodoxin reductase, and rat NADPH cytochrome P450 reductase were expressed in *Escherichia coli* and purified as described (31, 50–54). Incubations with CYP27A1 were as described (33) and contained the following reagent concentrations: 40 mM potassium phosphate buffer (KP_i, pH 7.2), 1 mM EDTA, 0.07 μM CYP27A1, 3.5 μM adrenodoxin, 0.35 μM adrenodoxin reductase, 50 μM cholestanol, and 1 mM NADPH. The assay conditions for CYP46A1 were as follows: 50 mM KP_i (pH 7.2), 100 mM NaCl, 0.02% CYMAL-6 (w/v), 40 μg of dilauroylglycerol 3-phosphatidylcholine, 0.5 μM CYP46A1, 1 μM NADPH cytochrome P450 reductase, 50 μM cholestanol, 2 units of catalase, and an NADPH-regenerating system (1 mM NADPH, 10 mM glucose-6-phosphate, and 2 units of glucose-6-phosphate dehydroge-

nase) (54). Cholestanol for both enzyme assays was added from 5 mM stock in 45% aqueous 2-hydroxypropyl-β-cyclodextrin (w/v) (HPCD). Sterols were extracted by dichloromethane (55) and analyzed by GC-MS (34).

Spectral Binding Assays—Titrations and data analysis were carried out as described (33, 54). The truncated, Δ(2–50), form of CYP46A1 was used, whose binding of substrates is similar to that of full-length enzyme (31). CYP46A1 (0.4 μM) was titrated at 24 °C in 1 ml of 50 mM KP_i (pH 7.2), containing 100 mM NaCl and 40 μg of dilauroylglycerol 3-phosphatidylcholine. Cholesterol or cholestanol was added from 0.5 mM stocks in 4.5% (w/v) aqueous HPCD. CYP27A1 (0.4 μM) was titrated at 30 °C in 1 ml of 50 mM KP_i (pH 7.2), containing 20% glycerol (v/v) and 500 mM KCl. Cholesterol or cholestanol were added from 0.25 mM stocks in 4.5% aqueous HPCD (w/v). Apparent binding constants (K_d) were calculated using either of the following equations,

$$\Delta A = (\Delta A_{max}[L]/(K_d + [L])) \quad \text{(Eq. 1)}$$

$$\Delta A = 0.5\Delta A_{max}(K_d + [E] + [L] - \sqrt{(K_d + [E] + [L]^2 - 4[E][L])} \quad \text{(Eq. 2)}$$

in which [E] is the enzyme concentration; ΔA is the spectral response at different ligand (sterol) concentrations [L], and ΔA_{max} is the maximal amplitude of the spectral response.

Statistics—Data represent mean ± S.D. Comparisons of sterol measurements were made by first performing a two-way analysis of variance in the Minitab statistical software package to assess for differences based on genotype, gender, and the interaction between genotype and gender. If significant differences were found based on the interaction between genotype and gender, then the individual main effects of genotype and gender were ignored. If the interaction between genotype and gender was not significant, pairwise comparisons were made based on genotype only using Bonferroni correction when data were collapsed across genders. p values for specific pairs were adjusted further by multiplying each by K/N. K is the number of biologically appropriate pairwise comparisons, namely comparisons between (i) knock-out mice of both genders and their corresponding wild type controls; (ii) knock-out mice of one gender and their corresponding wild type control; or (iii) female and male mice of the same genotype. N represents the total number of possible pairwise comparisons and was dependent on the number of genotypes in which each sterol could be detected. Statistical significance was defined as follows: *, $p \leq 0.05$; **, $p \leq 0.01$; ***, $p \leq 0.001$; and ****, $p \leq 0.0001$.

Author Contributions—N. M., K. W. A., J. B. L., and Y. L. conducted experiments; I. V. T., I. B., C. T., and I. A. P. analyzed the data; I. A. P. and I. B. designed experiments and wrote the manuscript.

Acknowledgments—We thank Dr. Pier Luigi DiPatre for obtaining human specimens and the NEI P30 Core Grant Facility for assistance with mouse breeding (Heather Butler and Kathryn Franke) and animal genotyping (John Denker).

References

1. Seyama, Y. (2003) Cholestanol metabolism, molecular pathology, and nutritional implications. *J. Med. Food.* **6,** 217–224
2. Bhattacharyya, A. K., Lin, D. S., and Connor, W. E. (2007) Cholestanol metabolism in patients with cerebrotendinous xanthomatosis: absorption, turnover, and tissue deposition. *J. Lipid Res.* **48,** 185–192
3. Bogaert, L. v., Scherer, H. J., Froelich, A., and Epstein, E. (1937) Une deuxieme observation de cholesterinose tendineuse symetrique avec symptomes cerebraux. *Ann. Med.* **42,** 69
4. Björkhem, I. (2013) Cerebrotendinous xanthomatosis. *Curr. Opin. Lipidol.* **24,** 283–287
5. Oftebro, H., Björkhem, I., Skrede, S., Schreiner, A., and Pederson, J. I. (1980) Cerebrotendinous xanthomatosis: a defect in mitochondrial 26-hydroxylation required for normal biosynthesis of cholic acid. *J. Clin. Invest.* **65,** 1418–1430
6. Cali, J. J., Hsieh, C. L., Francke, U., and Russell, D. W. (1991) Mutations in the bile acid biosynthetic enzyme sterol 27-hydroxylase underlie cerebrotendinous xanthomatosis. *J. Biol. Chem.* **266,** 7779–7783
7. Wikvall, K. (1984) Hydroxylations in biosynthesis of bile acids: isolation of a cytochrome P-450 from rabbit liver mitochondria catalyzing 26-hydroxylation of C27-steroids. *J. Biol. Chem.* **259,** 3800–3804
8. Masumoto, O., Ohyama, Y., and Okuda, K. (1988) Purification and characterization of vitamin D 25-hydroxylase from rat liver mitochondria. *J. Biol. Chem.* **263,** 14256–14260
9. Skrede, S., and Bjørkhem, I. (1985) A novel route for the biosynthesis of cholestanol, and its significance for the pathogenesis of cerebrotendinous xanthomatosis. *Scand. J. Clin. Lab. Invest. Suppl.* **177,** 15–21
10. Båvner, A., Shafaati, M., Hansson, M., Olin, M., Shpitzen, S., Meiner, V., Leitersdorf, E., and Björkhem, I. (2010) On the mechanism of accumulation of cholestanol in the brain of mice with a disruption of sterol 27-hydroxylase. *J. Lipid Res.* **51,** 2722–2730
11. Skrede, S., Björkhem, I., Buchmann, M. S., Hopen, G., and Fausa, O. (1985) A novel pathway for biosynthesis of cholestanol with 7α-hydroxylated C27-steroids as intermediates, and its importance for the accumulation of cholestanol in cerebrotendinous xanthomatosis. *J. Clin. Invest.* **75,** 448–455
12. Skrede, S., Björkhem, I., Buchmann, M. S., and Midtvedt, T. (1985) Biosynthesis of cholestanol from bile acid intermediates in the rabbit and the rat. *J. Biol. Chem.* **260,** 77–81
13. Björkhem, I., Skrede, S., Buchmann, M. S., East, C., and Grundy, S. (1987) Accumulation of 7α-hydroxy-4-cholesten-3-one and cholesta-4,6-dien-3-one in patients with cerebrotendinous xanthomatosis: effect of treatment with chenodeoxycholic acid. *Hepatology* **7,** 266–271
14. Panzenboeck, U., Andersson, U., Hansson, M., Sattler, W., Meaney, S., and Björkhem, I. (2007) On the mechanism of cerebral accumulation of cholestanol in patients with cerebrotendinous xanthomatosis. *J. Lipid Res.* **48,** 1167–1174
15. Björkhem, I., and Hansson, M. (2010) Cerebrotendinous xanthomatosis: an inborn error in bile acid synthesis with defined mutations but still a challenge. *Biochem. Biophys. Res. Commun.* **396,** 46–49
16. Björkhem, I., and Karlmar, K. E. (1974) Biosynthesis of cholestanol: conversion of cholesterol into 4-cholesten-3-one by rat liver microsomes. *Biochim. Biophys. Acta* **337,** 129–131
17. Buchmann, M. S., Björkhem, I., and Skrede, S. (1987) Metabolism of the cholestanol precursor cholesta-4,6-dien-3-one in different tissues. *Biochim. Biophys. Acta* **922,** 111–117
18. Skrede, S., Buchmann, M. S., and Björkhem, I. (1988) Hepatic 7α-dehydroxylation of bile acid intermediates, and its significance for the pathogenesis of cerebrotendinous xanthomatosis. *J. Lipid Res.* **29,** 157–164
19. Björkhem, I., Buchmann, M., and Byström, S. (1992) Mechanism and stereochemistry in the sequential enzymatic saturation of the two double bonds in cholesta-4,6-dien-3-one. *J. Biol. Chem.* **267,** 19872–19875
20. Puglielli, L., Friedlich, A. L., Setchell, K. D., Nagano, S., Opazo, C., Cherny, R. A., Barnham, K. J., Wade, J. D., Melov, S., Kovacs, D. M., and Bush, A. I. (2005) Alzheimer disease β-amyloid activity mimics cholesterol oxidase. *J. Clin. Invest.* **115,** 2556–2563

21. Jack, C. R., Jr., Wiste, H. J., Weigand, S. D., Knopman, D. S., Vemuri, P., Mielke, M. M., Lowe, V., Senjem, M. L., Gunter, J. L., Machulda, M. M., Gregg, B. E., Pankratz, V. S., Rocca, W. A., and Petersen, R. C. (2015) Age, sex, and ApoE $\epsilon4$ effects on memory, brain structure, and β-amyloid across the adult life span. *JAMA Neurol.* **72,** 511–519
22. Saadane, A., Mast, N., Charvet, C. D., Omarova, S., Zheng, W., Huang, S. S., Kern, T. S., Peachey, N. S., and Pikuleva, I. A. (2014) Retinal and non-ocular abnormalities in Cyp27a1$^{-/-}$ Cyp64a1$^{-/-}$ mice with dysfunctional metabolism of cholesterol. *Am. J. Pathol.* **184,** 2403–2419
23. Lütjohann, D., Breuer, O., Ahlborg, G., Nennesmo, I., Sidén, A., Diczfalusy, U., and Björkhem, I. (1996) Cholesterol homeostasis in human brain: evidence for an age-dependent flux of 24*S*-hydroxycholesterol from the brain into the circulation. *Proc. Natl. Acad. Sci. U.S.A.* **93,** 9799–9804
24. Lund, E. G., Guileyardo, J. M., and Russell, D. W. (1999) cDNA cloning of cholesterol 24-hydroxylase, a mediator of cholesterol homeostasis in the brain. *Proc. Natl. Acad. Sci. U.S.A.* **96,** 7238–7243
25. Liao, W. L., Heo, G. Y., Dodder, N. G., Reem, R. E., Mast, N., Huang, S., Dipatre, P. L., Turko, I. V., and Pikuleva, I. A. (2011) Quantification of cholesterol-metabolizing P450s Cyp27a1 and Cyp46a1 in neural tissues reveals a lack of enzyme-product correlations in human retina but not human brain. *J. Proteome Res.* **10,** 241–248
26. Heverin, M., Meaney, S., Lütjohann, D., Diczfalusy, U., Wahren, J., and Björkhem, I. (2005) Crossing the barrier: net flux of 27-hydroxycholesterol into the human brain. *J. Lipid Res.* **46,** 1047–1052
27. Meaney, S., Heverin, M., Panzenboeck, U., Ekström, L., Axelsson, M., Andersson, U., Diczfalusy, U., Pikuleva, I., Wahren, J., Sattler, W., and Björkhem, I. (2007) Novel route for elimination of brain oxysterols across the blood-brain barrier: conversion into 7α-hydroxy-3-oxo-4-cholestenoic acid. *J. Lipid Res.* **48,** 944–951
28. Rosen, H., Reshef, A., Maeda, N., Lippoldt, A., Shpizen, S., Triger, L., Eggertsen, G., Björkhem, I., and Leitersdorf, E. (1998) Markedly reduced bile acid synthesis but maintained levels of cholesterol and vitamin D metabolites in mice with disrupted sterol 27-hydroxylase gene. *J. Biol. Chem.* **273,** 14805–14812
29. Honda, A., Salen, G., Matsuzaki, Y., Batta, A. K., Xu, G., Leitersdorf, E., Tint, G. S., Erickson, S. K., Tanaka, N., and Shefer, S. (2001) Differences in hepatic levels of intermediates in bile acid biosynthesis between Cyp27$^{-/-}$ mice and CTX. *J. Lipid Res.* **42,** 291–300
30. Mast, N., Norcross, R., Andersson, U., Shou, M., Nakayama, K., Bjorkhem, I., and Pikuleva, I. A. (2003) Broad substrate specificity of human cytochrome P450 46a1 which initiates cholesterol degradation in the brain. *Biochemistry* **42,** 14284–14292
31. White, M. A., Mast, N., Bjorkhem, I., Johnson, E. F., Stout, C. D., and Pikuleva, I. A. (2008) Use of complementary cation and anion heavy-atom salt derivatives to solve the structure of cytochrome P450 46a1. *Acta Crystallogr. D Biol. Crystallogr.* **64,** 487–495
32. von Bahr, S., Movin, T., Papadogiannakis, N., Pikuleva, I., Rönnow, P., Diczfalusy, U., and Björkhem, I. (2002) Mechanism of accumulation of cholesterol and cholestanol in tendons and the role of sterol 27-hydroxylase (Cyp27a1). *Arterioscler. Thromb. Vasc. Biol.* **22,** 1129–1135
33. Mast, N., Murtazina, D., Liu, H., Graham, S. E., Bjorkhem, I., Halpert, J. R., Peterson, J., and Pikuleva, I. A. (2006) Distinct binding of cholesterol and 5-cholestane-3α,7α,12α-triol to cytochrome P450 27a1: evidence from modeling and site-directed mutagenesis studies. *Biochemistry* **45,** 4396–4404
34. Mast, N., Reem, R., Bederman, I., Huang, S., DiPatre, P. L., Bjorkhem, I., and Pikuleva, I. A. (2011) Cholestenoic acid is an important elimination product of cholesterol in the retina: comparison of retinal cholesterol metabolism with that in the brain. *Invest. Ophthalmol. Vis. Sci.* **52,** 594–603
35. Ramirez, D. M., Andersson, S., and Russell, D. W. (2008) Neuronal expression and subcellular localization of cholesterol 24-hydroxylase in the mouse brain. *J. Comp. Neurol.* **507,** 1676–1693
36. Pfrieger, F. W., and Ungerer, N. (2011) Cholesterol metabolism in neurons and astrocytes. *Prog. Lipid Res.* **50,** 357–371
37. Lund, E. G., Xie, C., Kotti, T., Turley, S. D., Dietschy, J. M., and Russell, D. W. (2003) Knockout of the cholesterol 24-hydroxylase gene in mice reveals a brain-specific mechanism of cholesterol turnover. *J. Biol. Chem.* **278,** 22980–22988
38. Pfrieger, F. W. (2003) Outsourcing in the brain: do neurons depend on cholesterol delivery by astrocytes? *Bioessays* **25,** 72–78
39. Vogel, M. W., Sunter, K., and Herrup, K. (1989) Numerical matching between granule and purkinje cells in lurcher chimeric mice: a hypothesis for the trophic rescue of granule cells from target-related cell death. *J. Neurosci.* **9,** 3454–3462
40. Andersson, S., Davis, D. L., Dahlbäck, H., Jörnvall, H., and Russell, D. W. (1989) Cloning, structure, and expression of the mitochondrial cytochrome P-450 sterol 26-hydroxylase, a bile acid biosynthetic enzyme. *J. Biol. Chem.* **264,** 8222–8229
41. Zheng, W., Mast, N., Saadane, A., and Pikuleva, I. A. (2015) Pathways of cholesterol homeostasis in mouse retina responsive to dietary and pharmacologic treatments. *J. Lipid Res.* **56,** 81–97
42. Brown, M. S., and Goldstein, J. L. (2009) Cholesterol feedback: from Schoenheimer's bottle to Scap's Meladl. *J. Lipid Res.* **50,** S15–S27
43. Song, B. L., and DeBose-Boyd, R. A. (2004) Ubiquitination of 3-hydroxy-3-methylglutaryl-CoA reductase in permeabilized cells mediated by cytosolic E1 and a putative membrane-bound ubiquitin ligase. *J. Biol. Chem.* **279,** 28798–28806
44. Mignarri, A., Magni, A., Del Puppo, M., Gallus, G. N., Björkhem, I., Federico, A., and Dotti, M. T. (2016) Evaluation of cholesterol metabolism in cerebrotendinous xanthomatosis. *J. Inherit. Metab. Dis.* **39,** 75–83
45. Mast, N., Li, Y., Linger, M., Clark, M., Wiseman, J., and Pikuleva, I. A. (2014) Pharmacologic stimulation of cytochrome P450 46a1 and cerebral cholesterol turnover in mice. *J. Biol. Chem.* **289,** 3529–3538
46. Anderson, K. W., Mast, N., Hudgens, J. W., Lin, J. B., Turko, I. V., and Pikuleva, I. A. (2016) Mapping of the allosteric site in cholesterol hydroxylase Cyp46a1 for efavirenz, a drug that stimulates enzyme activity. *J. Biol. Chem.* **291,** 11876–11886
47. Dubrac, S., Lear, S. R., Ananthanarayanan, M., Balasubramaniyan, N., Bollineni, J., Shefer, S., Hyogo, H., Cohen, D. E., Blanche, P. J., Krauss, R. M., Batta, A. K., Salen, G., Suchy, F. J., Maeda, N., and Erickson, S. K. (2005) Role of Cyp27a in cholesterol and bile acid metabolism. *J. Lipid Res.* **46,** 76–85
48. Omarova, S., Charvet, C. D., Reem, R. E., Mast, N., Zheng, W., Huang, S., Peachey, N. S., and Pikuleva, I. A. (2012) Abnormal vascularization in mouse retina with dysregulated retinal cholesterol homeostasis. *J. Clin. Invest.* **122,** 3012–3023
49. Liao, W. L., and Turko, I. V. (2008) Strategy combining separation of isotope-labeled unfolded proteins and matrix-assisted laser desorption/ionization mass spectrometry analysis enables quantification of a wide range of serum proteins. *Anal. Biochem.* **377,** 55–61
50. Pikuleva, I. A., Björkhem, I., and Waterman, M. R. (1997) Expression, purification, and enzymatic properties of recombinant human cytochrome P450c27 (Cyp27). *Arch. Biochem. Biophys.* **343,** 123–130
51. Hanna, I. H., Teiber, J. F., Kokones, K. L., and Hollenberg, P. F. (1998) Role of the alanine at position 363 of cytochrome P450 2b2 in influencing the NADPH- and hydroperoxide-supported activities. *Arch. Biochem. Biophys.* **350,** 324–332
52. Sagara, Y., Hara, T., Ariyasu, Y., Ando, F., Tokunaga, N., and Horiuchi, T. (1992) Direct expression in *Escherichia coli* and characterization of bovine adrenodoxins with modified amino-terminal regions. *FEBS Lett.* **300,** 208–212
53. Sagara, Y., Wada, A., Takata, Y., Waterman, M. R., Sekimizu, K., and Horiuchi, T. (1993) Direct expression of adrenodoxin reductase in *Escherichia coli* and the functional characterization. *Biol. Pharm. Bull.* **16,** 627–630
54. Mast, N., Linger, M., Clark, M., Wiseman, J., Stout, C. D., and Pikuleva, I. A. (2012) *In silico* and intuitive predictions of Cyp46a1 inhibition by marketed drugs with subsequent enzyme crystallization in complex with fluvoxamine. *Mol. Pharmacol.* **82,** 824–834
55. Mast, N., Andersson, U., Nakayama, K., Bjorkhem, I., and Pikuleva, I. A. (2004) Expression of human cytochrome P450 46a1 in *Escherichia coli*: effects of N- and C-terminal modifications. *Arch. Biochem. Biophys.* **428,** 99–108